AD_____

Award Number: W81XWH-10-1-0558

TITLE: Characterizing and Targeting Replication Stress Response Defects in Breast Cancer.

PRINCIPAL INVESTIGATOR: Shiaw-Yih Lin, Ph.D.

CONTRACTING ORGANIZATION: University of Texas M. D. Anderson Cancer Center
Houston, TX 77030

REPORT DATE: August 2015

TYPE OF REPORT: Annual

PREPARED FOR: U.S. Army Medical Research and Materiel Command
Fort Detrick, Maryland 21702-5012

DISTRIBUTION STATEMENT: Approved for Public Release;
Distribution Unlimited

The views, opinions and/or findings contained in this report are those of the author(s) and should not be construed as an official Department of the Army position, policy or decision unless so designated by other documentation.

REPORT DOCUMENTATION PAGE

Form Approved
OMB No. 0704-0188

1. REPORT DATE	**2. REPORT TYPE:**	**3. DATES COVERED**
August 2015	Annual	15 July 2014- 14 July 2015

4. TITLE AND SUBTITLE

Characterizing and Targeting Replication Stress Response Defects in Breast Cancer

5a. CONTRACT NUMBER
W81XWH-10-1-0558

5b. GRANT NUMBER

5c. PROGRAM ELEMENT NUMBER

6. AUTHOR(S)

Chun-Jen Lin, Hui Dai, Ju-Seog Lee, Chun Li, Shiaw-Yih Lin

E-Mail: sylin@mdanderson.org

5d. PROJECT NUMBER

5e. TASK NUMBER

5f. WORK UNIT NUMBER

7. PERFORMING ORGANIZATION NAME(S) AND ADDRESS(ES)

University of Texas M. D. Anderson Cancer Center
1515 Holcombe Blvd.
Houston, TX 77030

8. PERFORMING ORGANIZATION REPORT NUMBER

9. SPONSORING / MONITORING AGENCY NAME(S) AND ADDRESS(ES)
U.S. Army Medical Research and Materiel Command
Fort Detrick, Maryland 21702-5012

10. SPONSOR/MONITOR'S ACRONYM(S)

11. SPONSOR/MONITOR'S REPORT NUMBER(S)

12. DISTRIBUTION / AVAILABILITY STATEMENT
Approved for Public Release; Distribution Unlimited

13. SUPPLEMENTARY NOTES

14. ABSTRACT

During the fifth year of this project, we have successfully verified AXL protein as a reliable membrane marker for replication stress response defect (RSRD) breast cancer cells and we demonstrated the potential to use isotope-labeled anti-human AXL antibody to detect RSRD breast cancer cells *in vivo*.

In addition, we have clearly demonstrated the *in vivo* therapeutic effects of MEK inhibitor, AZD6244, and ERK inhibitor, SCH772984 on targeting RSRD breast cancer cells in two xenograft mouse models.
.

15. SUBJECT TERMS
Replication stress response, AXL, AZD6244, SCH772984, hallow gold nanoparticle (HAuNS)

16. SECURITY CLASSIFICATION OF:			**17. LIMITATION OF ABSTRACT**	**18. NUMBER OF PAGES**	**19a. NAME OF RESPONSIBLE PERSON**
a. REPORT	**b. ABSTRACT**	**c. THIS PAGE**			USAMRMC
U	U	U	UU	9	**19b. TELEPHONE NUMBER** *(include area code)*

Table of Contents

INTRODUCTION

In both precancerous breast lesions and breast cancer, hyperproliferative activity due to oncogene activation or loss of tumor suppressor genes induces stalling and collapse of DNA replication forks, which in turn activates the replication stress response (RSR) to maintain genome integrity [1-4]. RSR is a subset of the DNA damage response that safeguards the replication process [5]; defects in RSR allow the survival and proliferation of genomically unstable cells, ultimately leading to breast cancer [4-6]. Since the initial RSR defects occur before cancer develops, RSR defects can serve as a powerful biomarker to predict the risk of cell transformation. Importantly, the presence of RSR defects distinguishes premalignant lesions and breast cancer from normal tissues, which makes these defects effective targets for both breast cancer prevention and breast cancer treatment. This project is to use cutting-edge technologies to characterize novel RSR genes and their functions in tumor suppression; identify gene signature and membrane proteins associated with defective RSR; identify drugs that target these defects; and develop RSR-defect-targeting nanoparticles for diagnostic imaging, prevention, and treatment of breast cancer. During the first four years of this project, we have validated TUSC4 as a novel RSR gene and a bona fide tumor suppressor gene in breast cancer, established an RSR-defect (RSRD) gene signature, developed nano-particles that attached to the cells expressing high level of RSRD membrane markers *in vitro*, and identified compound candidates that specific targeted on RSRD cells. Here, we further investigated if and how we can detect RSRD breast cancer cells *in vivo*, and we also successfully validated the effectiveness of our compound candidates on killing RSRD breast cancer cells. The progress of our fifth year research is described below.

BODY

The tasks involved in our fifth-year research include: Task 4a,b.

Task 4a. To develop nano-imaging technology to detect RSR-defective breast cancer cells through binding of nano-imaging particles to the RSR-defect-specific membrane proteins.

Previously, we have shown our success in developing antibody-conjugated hallow gold nanoparticle (HAuNS) to bind RSRD cells *in vitro*. We conjugated HAuNS with the antibodies against AXL and Jag1, two RSRD membrane markers that we identified, and demonstrated that both HAuNS-AXL and HAuNS-Jag1 but not HAuNS-IgG control particles can specifically detect RSRD breast cancer cells *in vitro.* Since the affinity of HAuNS-AXL particles to the RSRD cells was significantly higher than HAuNS-Jag1, we decided to focus on HAuNS-AXL particles for the further *in vivo* studies.

Our *in vivo* imaging experiments were delayed due to the move of our collaborator Dr. Chun Li's lab from the north campus to the south campus of our institution. After resuming our studies, we found that the detection of RSRD cells *in vivo* had become a major challenge because of the large size of HAuNS-AXL particles. These antibody-conjugated particles failed to effectively reach tumor cells in our xenograft mouse model. Instead, we found that HAuNS-AXL particles were mainly accumulated in liver and spleen of mice with only very limited trace of particles detected in tumors. The similar problem has been frequently reported in the field when various nanoparticles were delivered *in vivo* for targeting. Despite our efforts to reduce the size of HAuNS and try to improve tumor targeting efficiency, the results of tumor detection were still not significantly improved.

While we continued to work on alternative strategies to develop appropriate vehicles for antibody delivery, we decided, at the same time, to determine if we can indeed detect RSRD cancer cells by anti-human AXL (hAXL) antibody in mice. To this end, we directly labeled isotope ^{64}Cu onto hAXL antibody or the control goat IgG. After labeling and purification process, the purity of ^{64}Cu-DOTA-hAXL and ^{64}Cu-DOTA-IgG could reach 96% and 89%, respectively (Figure 1). DOTA (1,4,7,10-

tetraazacyclododecane-1,4,7,10-tetraacetic acid) is an organic chelator that can trap isotope for labeling.

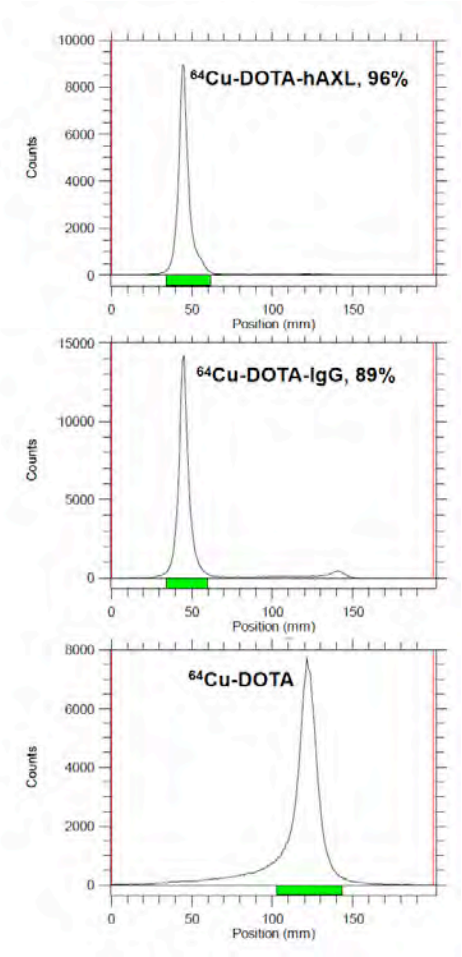

Figure 1. The purity of ^{64}Cu-DOTA-hAXL and ^{64}Cu-DOTA-IgG. The purity of ^{64}Cu-labeled hAXL and IgG were measured by thin-layer chromatography.

We next tested if the ^{64}Cu-labeled hAXL antibody can detect RSRD cancer cells in a mammary tumor xenograft model. We injected exponentially growing MDA-MB-231 (an RSRD breast cancer cell line) cells in the mammary fat pads of female nude mice. After the tumors developed, the labeled antibodies were delivered into mice through tail vein injection. As shown in the Figure 2, the ^{64}Cu-DOTA-hAXL showed a high efficiency and specificity in detecting tumors (right) and the negative control ^{64}Cu-DOTA-IgG didn't detect tumors (left).

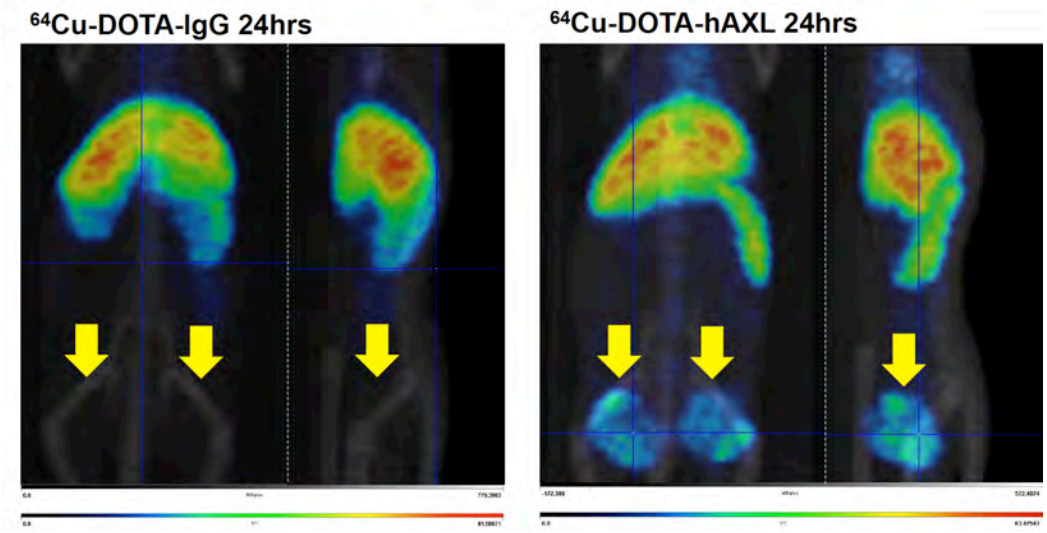

Figure. 2. ^{64}Cu-DOTA-hAXL specifically detects RSRD tumors in mice. The PET/CT images of ^{64}Cu-DOTA-hAXL and ^{64}Cu-DOTA-IgG on the detection of MDA-MB-231 xenograft tumors. Yellow arrows indicate tumor location.

We also performed bio-distribution assay to measure the level of ^{64}Cu-labeled hAXL and IgG in the organs and tumors (Figure 3A). Although both the labeled antibodies were highly accumulated in liver and spleen as expected, the MDA-MB-231 xenograft tumors only uptook ^{64}Cu-DOTA-hAXL but not ^{64}Cu-DOTA-IgG (Figure 3B, $P < 0.001$). These encouraging results confirmed the effectiveness of AXL as an RSRD marker and revealed the potential to use the isotope-labeled AXL antibody to detect RSRD tumors in clinic in the future. In the following year, we will continue to work on various strategies to reduce the size of hAXL-conjugated HAuNS such as through fragmentation of hAXL antibody with the goal to achieve the same detection power on RSRD breast tumors as hAXL antibody alone.

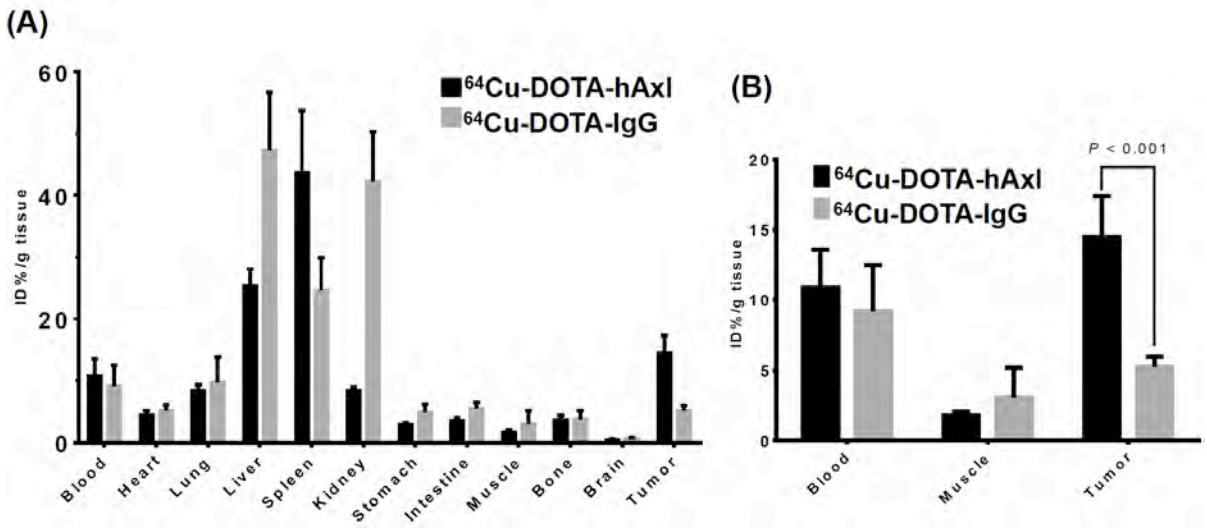

Figure 3. The bio-distribution of ^{64}Cu-DOTA-hAXL and ^{64}Cu-DOTA-IgG in RSRD mammary xenograft mouse model (A) The distribution of ^{64}Cu-DOTA-hAXL and ^{64}Cu-DOTA-IgG in the organs and tumors of MDA-MB-231 xenograft mice 24 hours after intravenous injection. The results were measured by percentage of the injected dose per gram of tissue (%ID/g). Error bar indicates mean ± SEM (n=3). (B) The uptake of ^{64}Cu-DOTA-hAXL and ^{64}Cu-DOTA-IgG in MDA-MB-231 xenograft tumors 24 hours after intravenous injection. The (%ID/g) in blood and muscle are used as the negative controls.

Task 4b. To develop nanoparticles to kill RSR-defective breast cancer cells through their binding to the RSR-defect-specific membrane proteins on cancer cells.

As described in our fourth year progress report, in addition to MEK inhibitors (e.g., AZD6244), we identified ERK inhibitors (e.g., SCH772984) as effective agents to kill RSRD breast cancer cells *in vitro*. During the fifth year of the award period, we further assessed the therapeutic effects of both AZD6244 and SCH772984 on RSRD breast cancer *in vivo* using two breast cell xenograft models (4A, 4B). We injected exponentially growing MDA-MB-231 cells or MCF-10A_HRas^{V12G} cells in the mammary fat pads of female nude mice. MDA-MB-231 is a well characterized RSRD breast cancer line. MCF-10A_HRas^{V12G} is an MCF-10A derivative line that we have generated. This cell line contains a doxycycline-inducible HRas^{V12G} expression construct and an shRNA construct that stably knocks down key RSR genes (i.e., ATM, ATR, Chk1 and Chk2).

These mice were randomized and subjected to the treatment of vehicle (methocel/polysorbate buffer), AZD6244 (100 mg/kg), or SCH772984 (40 mg/kg). We then measured the tumors via digital caliper to

determine the tumor volume using the formula [L/2] x [W2], where L represents length and is the largest value and W represents width and is the smallest value. As shown in the Figure 4C, left panels and 4D, left panels, AZD6244 and SCH772984 treatments significantly prevented tumor formation in both RSRD tumor models. We also measured the body weight of mice and found no detectable side effect on mice from all these treatments (Figure 4C and 4D, right panels). Together, our results (summarized in Table 1 and 2 below) clearly confirmed the great therapeutic potential of AZD6244 and SCH772984 on treating or even preventing RSRD breast cancer. In the following year, we will conjugate these two drugs onto HAuNS-AXL particles and test their *in vivo* targeting effects once we resolve the *in vivo* delivery problem of HAuNS-AXL particles described above.

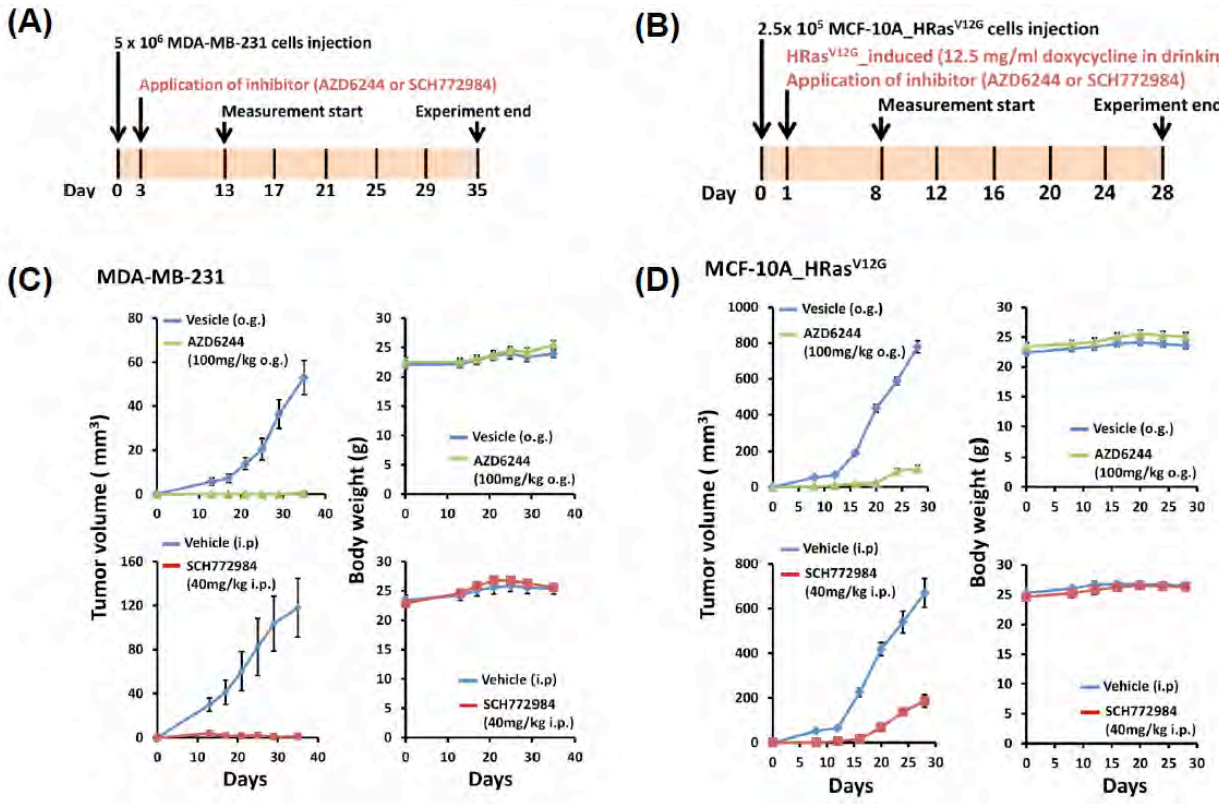

Figure 4. MEK or ERK inhibitor effectively prevents early tumorigenesis *in vivo*. (A and B) Experimental design of MDA-MB-231 or MCF-10A_HRas^{V12G}-induced xenograft model with vehicle, AZD6244, or SCH772984 treatment. (C and D) Mean tumor volume (± SEM) and mean body weight (± SEM) was measured in either MDA-MB-231 or MCF-10A_HRas^{V12G}-induced xenograft model upon vehicle, AZD6244, or SCH772984 treatment. $P < 0.05$ compared with vehicle treatment (2-tailed t-test). o.g., oral gavage. i.p., intraperitoneal injection. N = 8.

Table 1. The summary of tumorigenesis assay in MDA-MB-231 xenograft model

Xenograft model	MDA-MB-231 xenograft model						
Treatment	Vehicle (o. g)						
Days	0	13	17	21	25	29	35
mice with tumor/total mice	6/10	8/10	10/10	10/10	10/10	10/10	10/10
Avg. tumor volumn (mm^3)	0.0 ± 0.0	5.7 ± 1.8	7.2 ± 1.9	13.8 ± 2.7	20.4 ± 4.9	36.4 ± 6.5	53.0 ± 7.8
Avg. body weight (g)	22.1 ± 0.6	22.1 ± 0.7	22.8 ± 0.7	23.7 ± 0.8	23.9 ± 0.8	23.4 ± 0.8	23.9 ± 0.7
Xenograft model	MDA-MB-231 xenograft model						
Treatment	AZD6244 (100 mg/kg o. g)						
Days	0	13	17	21	25	29	35
mice with tumor/total mice	0/10	0/10	0/10	0/10	0/10	0/10	1/10
Avg. tumor volumn (mm^3)	0.0 ± 0.0	0.0 ± 0.0	0.0 ± 0.0	0.0 ± 0.0	0.0 ± 0.0	0.0 ± 0.0	0.4 ± 0.4
Avg. body weight (g)	22.5 ± 0.7	22.5 ± 0.6	23.1 ± 0.6	23.7 ± 0.6	24.6 ± 0.6	24.2 ± 0.7	25.5 ± 0.7

Xenograft model	MDA-MB-231 xenograft model						
Treatment	Vehicle (i. p)						
Days	0	13	17	21	25	29	35
mice with tumor/total mice	8/8	8/8	8/8	8/8	8/8	8/8	8/8
Avg. tumor volumn (mm^3)	0.0 ± 0.0	29.9 ± 6.1	41.3 ± 10.9	60.4 ± 17.8	82.3 ± 25.9	103.6 ± 25.0	118.0 ± 26.7
Avg. body weight (g)	23.5 ± 0.6	24.2 ± 0.6	25.1 ± 0.5	25.6 ± 0.5	25.9 ± 0.5	25.5 ± 0.6	25.4 ± 0.7
Xenograft model	MDA-MB-231 xenograft model						
Treatment	SCH772984 (40 mg/kg i. p)						
Days	0	13	17	21	25	29	35
mice with tumor/total mice	0/8	2/8	2/8	2/8	2/8	1/8	1/8
Avg. tumor volumn (mm^3)	0.0 ± 0.0	2.0 ± 1.3	1.8 ± 1.2	1.6 ± 1.1	1.9 ± 1.3	1.0 ± 1.0	1.1 ± 1.1
Avg. body weight (g)	22.9 ± 0.9	24.6 ± 0.8	25.8 ± 1.0	26.8 ± 1.1	26.8 ± 1.0	26.3 ± 1.0	25.6 ± 0.9

Table 2. The summary of tumorigenesis assay in MCF10A_HRas^{V12G}-induced xenograft model

Xenograft model	MCF-10A_HRas^{V12G}-induced xenograft model						
Treatment	Vehicle (o. g)						
Days	0	8	12	16	20	24	28
mice with tumor/total mice	0/8	8/8	8/8	8/8	8/8	8/8	8/8
Avg. tumor volumn (mm^3)	0.0 ± 0.0	54.0 ± 3.2	66.3 ± 6.2	190.7 ± 10.6	435.4 ± 21.7	587.2 ± 23.2	779.2 ± 33.8
Avg. body weight (g)	22.4 ± 0.5	23.1 ± 0.5	23.4 ± 0.5	23.9 ± 0.5	24.2 ± 0.5	23.9 ± 0.5	23.6 ± 0.6
Xenograft model	MCF-10A_HRas^{V12G}-induced xenograft model						
Treatment	AZD6244 (100 mg/kg o. g)						
Days	0	8	12	16	20	24	28
mice with tumor/total mice	0/8	7/8	8/8	8/8	8/8	8/8	8/8
Avg. tumor volumn (mm^3)	0.0 ± 0.0	3.9 ± 1.2	9.6 ± 1.5	18.25 ± 1.4	21.5 ± 1.8	89.6 ± 16.1	104.8 ± 18.1
Avg. body weight (g)	23.4 ± 0.6	23.9 ± 0.6	24.2 ± 0.6	25.1 ± 0.6	25.6 ± 0.7	25.3 ± 0.7	25.1 ± 0.7

Xenograft model	MCF-10A_HRas^{V12G}-induced xenograft model						
Treatment	Vehicle (i. p)						
Days	0	8	12	16	20	24	28
mice with tumor/total mice	0/8	8/8	8/8	8/8	8/8	8/8	8/8
Avg. tumor volumn (mm^3)	0.0 ± 0.0	52.2 ± 6.7	65.6 ± 10.4	224.9 ± 19.6	418.2 ± 29.2	540.8 ± 49.2	670.0 ± 64.7
Avg. body weight (g)	25.3 ± 0.3	26.1 ± 0.5	26.7 ± 0.5	26.7 ± 0.5	26.7 ± 0.4	26.7 ± 0.4	26.6 ± 0.5
Xenograft model	MCF-10A_HRas^{V12G}-induced xenograft model						
Treatment	SCH772984 (40 mg/kg i. p)						
Days	0	8	12	16	20	24	28
mice with tumor/total mice	0/8	2/8	8/8	8/8	8/8	8/8	8/8
Avg. tumor volumn (mm^3)	0.0 ± 0.0	0.3 ± 0.2	6.2 ± 1.5	17.5 ± 4.4	67.4 ± 8.3	137.2 ± 18.1	186.5 ± 28.2
Avg. body weight (g)	24.6 ± 0.7	25.2 ± 0.8	25.8 ± 0.8	26.3 ± 0.7	26.6 ± 0.6	26.4 ± 0.7	26.3 ± 0.6

KEY RESEARCH ACCOMPLISHMENTS

(1) We successfully labeled anti-human AXL antibody with isotope and demonstrated the effectiveness and specificity of AXL antibody in detecting RSRD breast cancer cells *in vivo.*
(2) We have successfully demonstrated very promising therapeutic effects of both MEK inhibitor (AZD6244) and ERK inhibitor (SCH772984) in treating RSRD breast tumors *in vivo* with no detectable side effect.

REPORTABLE OUTCOMES

The progress of this project in the past year has led to one manuscript under review in Journal of Clinical Investigation. Our findings have also allowed me to be invited for presentation at SCBA The 15th International Symposium in Taiwan, and one poster presentation by my postdoctoral fellow at the Conference of Exploring DNA Repair Pathways as Targets for Cancer at Cancun, Mexico.

CONCLUSION

During the fifth year of this project, despite some delay due to the laboratory move of our collaborator and the challenge from achieving effective delivery of antibody-conjugated nano-particles, we have successfully verified AXL as a reliable membrane marker for RSRD breast cancer cells and we demonstrated the potential to use isotope-labeled hAXL antibody to detect RSRD mammary tumors *in vivo*.

In addition, we have clearly demonstrated the *in vivo* therapeutic effects of MEK inhibitor, AZD6244 and ERK inhibitor, SCH772984 on targeting RSRD breast cancer cells in two xenograft mouse models.

REFERENCES

1. Bartkova J, Horejsí Z, Koed K, Krämer A, Tort F, Zieger K, Guldberg P, Sehested M, Nesland JM, Lukas C, Ørntoft T, Lukas J, Bartek J. (2005) DNA damage response as a candidate anti-cancer barrier in early human tumorigenesis. Nature. *434*:864-870.
2. Bartkova J, Rezaei N, Liontos M, KaTUSC4aidos P, Kletsas D, Issaeva N. et al., (2006) Oncogene-induced senescence is part of the tumorigenesis barrier imposed by DNA damage checkpoints. Nature *444*:633-637.
3. Di Micco R, Fumagalli M, Cicalese A, Piccinin S, Gasparini P et al., (2006) Oncogene-induced senescence is a DNA damage response triggered by DNA hyper-replication. Nature *444:* 638-642.
4. Halazonetis TD, Gorgoulis VG, Bartek J. (2008) An oncogene-induced DNA damage model for cancer development. Science *319*:1352-1355.
5. Osborn AJ, Elledge SJ, Zou L. (2006) Checking on the fork: the DNA-replication stress-response pathway. Trends Cell Biol. *12(11*):509-516.
6. Dapic V, Carvalho MA, Monteiro AN. (2005) Breast cancer susceptibility and the DNA damage response. Cancer Control *12*:127-136.